

On the cylindrically symmetric wormholes WhCR^e: The motion of test particles.

Asya V. Aminova* and Pavel I. Chumarov†

*Department of General Relativity and Gravitation,
Kazan Federal University, 18 Kremlyovskaya St., Kazan 420008, Russia*

Dieter R. Brill‡

Maryland Center for Fundamental Physics, University of Maryland, College Park, MD 20742, USA

Aleksandr Yu. Shemakhin§

*Department of Radiophysics, Institute of Physics, Department of Mathematical Statistics,
Institute of Computer Mathematics and Information Technologies,
Kazan Federal University, 18 Kremlyovskaya St., Kazan 420008, Russia*

In this article we partially implement the program outlined in the previous paper of the authors [5]. The program owes its origins to the following comment in paper [1], where a class of static spherically symmetric solutions in $(4+n)$ -dimensional Kaluza–Klein theory was studied: “...We suspect that the same thing [as for spherical symmetry] will happen for axially symmetric stationary configurations, but it remains to be proven”. We study the radial and non-radial motion of test particles in the cylindrically symmetric wormholes found in [5] of type WhCR^e in 6-dimensional reduced Kaluza–Klein theory with Abelian gauge field and two dilaton fields, with particular attention to the extent to which the wormhole is traversable. In the case of non-radial motion along a hypersurface $z = \text{const}$ (“planar orbits”) we show that, as in the Kerr and Schwarzschild geometries [17], we should distinguish between orbits with impact parameters greater resp. less than a certain critical value D_c , which corresponds to the unstable circular orbit of radius u_c (r_c).¹ For $D^2 > D_c^2$ there are two kinds of orbits: orbits of the first kind arrive from infinity and have pericenter distances greater than u_c , whereas orbits of the second kind have apocenter distances less than u_c and terminate at the singularity at $u = -\infty$ ($r = 0$). For $D = D_c$ orbits of the first and second kinds merge and both orbits spiral an infinite number of times toward the unstable circular orbit $u = u_c$. For $D^2 < D_c^2$ we have only orbits of one kind: starting at infinity, they cross the wormhole throat and terminate at the singularity.

PACS numbers: 04.20.Jb 04.50.Cd

I. INTRODUCTION.

The general static cylindrically symmetric space-time metric can be written in the form

$$ds^2 = e^{2\gamma(u)} dt^2 - e^{2[\beta(u)+\gamma(u)+\xi(u)]} du^2 - e^{2\xi(u)} dz^2 - e^{2\beta(u)} d\phi^2, \quad (1)$$

where $u \in (-\infty, +\infty)$ is a cylindrical radial coordinate, $z \in (-\infty, +\infty)$ is the longitudinal coordinate, and $\phi \in [0, 2\pi]$ is the angular coordinate (see [3]).

The metric (1) has one timelike Killing vector $\xi_1 = \partial_t$ and two spacelike Killing vectors $\xi_2 = \partial_\phi$, $\xi_3 = \partial_z$, which define the axial symmetry. It is invariant under the simultaneous interchange $z \leftrightarrow \phi$ and $\xi \leftrightarrow \beta$; one of the coordinates (ϕ) was arbitrarily chosen to be periodic with period 2π to represent a cylindrically symmetric (rather than plane symmetric) geometry. (Frequently the scale of ϕ is chosen uniquely to make the origin nonsingular, but this cannot be done for the metrics considered here.)

Radial null geodesics are described by $du/dt = \pm e^{-(\beta(u)+\xi(u))}$, which will be non-zero for all u . Therefore there is no horizon, and any singularity at the origin is visible from everywhere (“naked”).

By definition, metric (1) describes a *cylindrically symmetric wormhole* V if the “circle radius” $\rho(u) := e^{\beta(u)}$ has an absolute minimum $\rho(u_0) > 0$ at some point $u = u_0$ and for all possible values of u the metric functions

¹ Note the difference in the notations: in [17] $u = 1/r$ where r is the radial spherical coordinate, here $u = \ln r$ where r is the radial cylindrical coordinate.

*Electronic address: asya.aminova@kpfu.ru

†Electronic address: p.i.t.choumarov@mail.ru

‡Electronic address: brill@umd.edu

§Electronic address: Aleksandr.Shemakhin@kpfu.ru

$\beta(u)$, $\gamma(u)$, and $\xi(u)$ are smooth and finite [3].

A cylindrical hypersurface Σ_0 defined by the equation $u = u_0$ is called a *throat* of the wormhole V , if V can be presented as the union $V = V_- \cup \Sigma_0 \cup V_+$, where $V_- = \{(t, u, z, \phi) \in V \mid u < u_0\}$ and $V_+ = \{(t, u, z, \phi) \in V \mid u > u_0\}$ are interpreted as the two universes at the ends of the wormhole.

The wormhole is called *traversable* if travel is possible from one universe (V_- or V_+) to another (V_+ or V_- , respectively), i.e., if a traversing timelike path through the wormhole's throat is allowed in a finite time (see, for example, [4]).

In [5] we studied cylindrically symmetric Abelian wormholes in $(4+n)$ -dimensional Kaluza-Klein theory. It was shown that static four-dimensional cylindrically symmetric solutions in $(4+n)$ -dimensional Kaluza-Klein theory with maximal Abelian isometry group $U(1)^n$ of the internal space with diagonal internal metric can be obtained (as in the case of a supersymmetric static black hole [2]) only if the isometry group of the internal space is broken down to the $U(1)_e \times U(1)_m$ gauge group; the solutions correspond to dyonic configurations with one electric (Q_e) and one magnetic (Q_m) charge that are related either to the same $U(1)_e$ or $U(1)_m$ gauge field or to different factors of the $U(1)_e \times U(1)_m$ gauge group of the effective six-dimensional Kaluza-Klein theory. We found new static cylindrically symmetric exact solutions of the six-dimensional Kaluza-Klein theory with two Abelian gauge fields A_μ , B_μ , a dilaton field ψ , and a scalar field χ associated with the internal metric. We obtained new types of static cylindrically symmetric wormholes supported by radial and longitudinal electric and magnetic fields. In the case of radial gauge fields we found three types of static cylindrically symmetric wormholes: dyonic $\text{WhCR}^{e;m}$ with nonzero electric and magnetic charges, WhCR^e with nonzero electric charge, and WhCR^m with nonzero magnetic charge. For longitudinal gauge fields we obtained nine types of dyonic wormholes $\text{WhCL}^{k|e;j|m}$, $k, j = 1, 2, 3$, the wormhole $\text{WhCL}^{3|e}$ with nonzero electric charge, and the wormhole $\text{WhCL}^{3|m}$ with nonzero magnetic charge. From the physical point of view these wormholes are interesting because they do not need exotic matter or phantom fields for support. However the universes V_- and V_+ at the ends of the wormhole are not benign, for example V_- contains a curvature singularity. We will leave exploration of these features to a later investigation and focus here primarily on the interesting, near-throat region.

In this article we consider the geodesic structure of the wormhole solutions of type WhCR^e with the space-time metric in coordinates $t, r = e^u, z, \phi$ ([5], Eqs. (35)-(38))

$$ds^2 = k_e \Lambda_e \left(\frac{r^{2c} dt^2}{k_e^2 \Lambda_e^2} - r^{2(a+b-c-1)} dr^2 - r^{2(b-c)} dz^2 - r^{2(a-c)} d\phi^2 \right) \quad (a, b, c = \text{const}),$$

where

$$k_e = \sqrt{|q_e|} \equiv \sqrt{|Q_e/h_e|}, \quad \Lambda_e = \sqrt{(r/r_e)^{h_e} + (r/r_e)^{-h_e}}, \quad 4ab = h_e^2 + 16c^2$$

$$(h_e, q_e = \text{const}, h_e q_e \neq 0).$$

The throat radius of the WhCR^e is

$$r_0 = r_e \left(\frac{h_e - 4(a-c)}{h_e + 4(a-c)} \right)^{1/(2h_e)}, \quad h_e > 4|a-c| > 0,$$

and the wormhole is generated by the following Abelian gauge field A_μ , dilaton ψ , and scalar field χ :

$$A_\mu = \left((-1/(4q_e)) [(r/r_e)^{h_e} - (r/r_e)^{-h_e}] [(r/r_e)^{h_e} + (r/r_e)^{-h_e}]^{-1}, 0, 0, 0 \right),$$

$$\psi = (1/(2\sqrt{2})) \ln (|q_e| r^{4c} [(r/r_e)^{h_e} + (r/r_e)^{-h_e}]),$$

$$\chi = -(1/(4\sqrt{2})) \ln (|q_e| r^{-4c} [(r/r_e)^{h_e} + (r/r_e)^{-h_e}]).$$

Further in this paper we put $r_e = 1, c = 0, h_e \equiv h$ and consider a 3-parameter family of the wormholes WhCR^e with the line interval

$$ds^2 = \frac{dt^2}{\sqrt{|q_e|} \sqrt{r^h + r^{-h}}} - \sqrt{|q_e|} \sqrt{r^h + r^{-h}} \left(r^{2(a+b-1)} dr^2 + r^{2b} dz^2 + r^{2a} d\phi^2 \right) \quad (2)$$

and the throat radius

$$r_0 = \left(\frac{1 - 4a/h}{1 + 4a/h} \right)^{1/(2h)}$$

defined in coordinates t, u, z, ϕ by the formulas:

$$ds^2 = \frac{dt^2}{\sqrt{2|q_e| \cosh(hu)}} - \sqrt{2|q_e| \cosh(hu)} \left(e^{2(a+b)u} du^2 + e^{2bu} dz^2 + e^{2au} d\phi^2 \right), \quad (3)$$

$$4ab = h^2 > 0, \quad 4|a| < h < b, \quad q_e \neq 0.$$

Further, we put $a > 0$, whence $b = h^2/(4a) > 0$, $4a/h < 1$, and $r_0 < 1$, since the opposite choice $a = -\alpha^2 < 0$, $b = -h^2(4\alpha^2)$ is reduced to the previous one by a change $r \rightarrow 1/r$. Metric (2) and its geodesics as well as dilaton field ψ and scalar field χ are invariant under this change, while the gauge field changes sign.

Metric (2) can be obtained from (1) by putting

$$\beta = au + \frac{1}{4} \ln(2|q_e| \cosh(hu)), \quad \gamma = -\frac{1}{4} \ln(2|q_e| \cosh(hu)), \quad \xi = bu + \frac{1}{4} \ln(2|q_e| \cosh(hu)). \quad (4)$$

The hypersurface

$$u = u_0 \equiv -h^{-1} \operatorname{arctanh}(4a/h) \quad (5)$$

is the throat of wormhole (3), which is generated by the following vector, dilaton, and scalar fields:

$$A_\mu = \left(-\frac{1}{4q_e} \tanh(hu), 0, 0, 0 \right), \quad \psi = -2\chi = \frac{1}{2\sqrt{2}} \ln(2|q_e| \cosh(hu)).$$

Note that metric (3) is not asymptotically flat, which confirms the “no-go” statement about the nonflat asymptotic behavior of a cylindrically symmetric wormhole in the absence of ghost fields, i.e., fields having negative kinetic energy [3].

As the main source of information about the structure of any physical field is the behavior of test bodies, we will focus on the motion of test particles in the wormhole WhCR^e whose trajectories are geodesics.

The geodesic motion in space-times of spherically symmetric wormholes [6] was studied, for example, in [4], [7].

In [4] a detailed derivation of solutions of the Einstein field equations was presented, which describe traversable wormholes that, in principle, could be traversed by human beings.

The creation of wormholes and their conversion into time machines as well as quantum-field-theoretic stress-energy tensors that are required to maintain a two-way traversable wormhole were discussed in [7].

In [8] the motion of massive and massless test particles in a space-time of a slowly rotating spherically symmetric wormhole with a ghost scalar field as a source was considered, and it was shown that after crossing the wormhole throat the particles (massive or massless) moving initially radially will move in a spiral away from the throat.

The study of dynamics of null and timelike geodesics for traversable static spherically symmetric Schwarzschild and Kerr thin-shell wormholes constructed by cut-and-paste method was presented in [9].

The radial geodesic motion of a massive particle into a version of an Einstein–Rosen bridge was considered in [10]. This wormhole was constructed by gluing regions I and III of the Kruskal space-time along the future resp. past horizons, which requires a delta-function matter source violating the energy conditions. This wormhole is traversable by complete timelike geodesics. The author suggests that observed astrophysical black holes may be Einstein–Rosen bridges, each with a new universe inside.

In [11] the geodesic motion of charged test particles in the gravitational field of a rotating and electromagnetically charged Kerr–Newman black hole was studied; the colatitudinal and radial motions of particles moving along timelike world lines were classified.

A class of axially symmetric stationary exact solutions of the phantom scalar field in general relativity describing rotating and magnetised wormholes was found in [12].

In [13] properties of a Kerr-like wormhole supported by phantom matter were studied. The geodesics of the Kerr-like phantom wormhole were analysed in [14], where it was shown that the wormhole can be traversable for an observer like a human being.

This article is organized as follows. In section II we discuss the general properties of geodesic motion in space-time (3). We compute Kretschmann’s invariant $K = R_{\mu\nu\lambda\rho} R^{\mu\nu\lambda\rho}$ and show that the space-time (3) becomes singular as $u \rightarrow -\infty$ and has a physical (naked) singularity at $u = -\infty$ (for $a, b > 0$). In section III we describe radial motion of massive test particles. We find the turning points u_\pm of the particle motion and the regions accessible by a particle with energy E . Equating u_- and u_+ , we find $u = 0$, $E = 1/\sqrt[4]{2|q_e|} \equiv E_0$. We prove that the particle located at $u = u_- = u_+ = 0$ will be at the point of unstable equilibrium and

study in detail the character of motion of particles with energies E greater and/or less than E_0 . We find a (lower) energy threshold $E_{thr} \equiv E_0 \sqrt[8]{1 - 16a^2/h^2}$ of traversability of the wormhole throat for a radially moving massive test particle. In section IV we consider radial trajectories of photons and prove that each of such trajectories crosses the throat. Non-radial motion along a hypersurface $z = \text{const}$ (“planar orbits”) is studied in section V where we draw parallels with the Kerr and Schwarzschild geometries. In section VI we investigate non-radial motion in the plane $\phi = \text{const}$. We prove that all null orbits have a pericenter distance u_1 and terminate at radial infinity and identify four types of massive particle behavior. Conclusions are given in section VII.

II. THE GENERAL PROPERTIES OF GEODESIC MOTION IN THE SPACE-TIME (1).

According to the general theory of relativity, trajectories $x^\mu = x^\mu(\tau)$ of test particles in the absence of force fields are geodesics, which are integral curves of the equations

$$\frac{Dv^\mu}{d\tau} \equiv \ddot{x}^\mu + \Gamma_{\nu\sigma}^\mu \dot{x}^\nu \dot{x}^\sigma = 0, \quad (6)$$

where $D/d\tau$ denotes the absolute derivative with respect to an affine parameter τ , $v^\mu := dx^\mu/d\tau$ is the 4-velocity vector of the test particle, $\Gamma_{\nu\sigma}^\mu$ are the Christoffel symbols, and overdots denote derivatives with respect to τ . For metric (1) the non-vanishing Christoffel symbols are

$$\begin{aligned} \Gamma_{tu}^t &= \gamma', \quad \Gamma_{tt}^u = e^{-2(\beta+\xi)}\gamma', \quad \Gamma_{uu}^u = \beta' + \gamma' + \xi', \\ \Gamma_{zz}^u &= -e^{-2(\beta+\gamma)}\xi', \quad \Gamma_{\phi\phi}^u = -e^{-2(\gamma+\xi)}\beta', \quad \Gamma_{uz}^z = \xi', \quad \Gamma_{\phi u}^\phi = \beta', \end{aligned}$$

and Eq. (6) gives

$$\dot{v}^t + 2\gamma' v^t v^u = 0, \quad (7)$$

$$\dot{v}^u + (\beta' + \gamma' + \xi')(v^u)^2 + \gamma' e^{-2(\beta+\xi)}(v^t)^2 - \xi' e^{-2(\beta+\gamma)}(v^z)^2 - \beta' e^{-2(\gamma+\xi)}(v^\phi)^2 = 0, \quad (8)$$

$$\dot{v}^z + 2\xi' v^z v^u = 0, \quad (9)$$

$$\dot{v}^\phi + 2\beta' v^\phi v^u = 0 \quad (10)$$

($v^t \equiv \dot{t}$, $v^u \equiv \dot{u}$, $v^z \equiv \dot{z}$, $v^\phi \equiv \dot{\phi}$, and the prime denotes the derivative with respect to the radial coordinate u).

The equations of motion can also be obtained from the Lagrangian

$$\mathcal{L} = \frac{1}{2} g_{\mu\nu} \dot{x}^\mu \dot{x}^\nu \equiv \frac{1}{2} \left(e^{2\gamma} \dot{t}^2 - e^{2(\beta+\gamma+\xi)} \dot{u}^2 - e^{2\xi} \dot{z}^2 - e^{2\beta} \dot{\phi}^2 \right).$$

The canonical momenta are

$$\begin{aligned} p_t &\equiv \frac{\partial \mathcal{L}}{\partial \dot{t}} = e^{2\gamma} \dot{t}, \quad p_u \equiv \frac{\partial \mathcal{L}}{\partial \dot{u}} = -e^{2(\beta+\gamma+\xi)} \dot{u}, \\ p_z &\equiv \frac{\partial \mathcal{L}}{\partial \dot{z}} = -e^{2\xi} \dot{z}, \quad p_\phi \equiv \frac{\partial \mathcal{L}}{\partial \dot{\phi}} = -e^{2\beta} \dot{\phi}, \end{aligned} \quad (11)$$

and the Hamiltonian function is $H = v^\mu p_\mu - \mathcal{L} = \mathcal{L}$. From the Hamilton's equations $\dot{p}_\mu = -\partial H / \partial x^\mu$ we find

$$\dot{p}_t = -\frac{\partial \mathcal{L}}{\partial t} = 0, \quad \dot{p}_z = -\frac{\partial \mathcal{L}}{\partial z} = 0, \quad \dot{p}_\phi = -\frac{\partial \mathcal{L}}{\partial \phi} = 0.$$

By integrating, we obtain first integrals of the geodesic equations (6) in the cylindrically symmetric space-time (1):

$$p_t = e^{2\gamma} \dot{t} \equiv E = \text{const} > 0, \quad p_z = -e^{2\xi} \dot{z} \equiv -M_z = \text{const}, \quad p_\phi = -e^{2\beta} \dot{\phi} \equiv -L = \text{const}. \quad (12)$$

They are generated by the three Killing vector fields $\partial/\partial t$, $\partial/\partial z$, and $\partial/\partial \phi$. The constants of motion E and L are interpreted as the energy and angular momenta per unit mass of the particle with non-zero rest mass.

From Eq. (12) we have

$$t(\tau) = t_0 + E \int_{\tau_0}^{\tau} e^{-2\gamma(u(\bar{\tau}))} d\bar{\tau}, \quad z(\tau) = z_0 + M_z \int_{\tau_0}^{\tau} e^{-2\xi(u(\bar{\tau}))} d\bar{\tau}, \quad \phi(\tau) = \phi_0 + L \int_{\tau_0}^{\tau} e^{-2\beta(u(\bar{\tau}))} d\bar{\tau}, \quad (13)$$

here τ_0 denotes the initial value of the parameter τ and the integration constants t_0 , z_0 , and ϕ_0 are the initial values of the coordinates t , z , and ϕ , respectively.

From Eq. (12) and the equality $v_\mu v^\mu = \iota$, where $\iota = 1$ for time-like geodesics and $\iota = 0$ for null geodesics, we get

$$\dot{u}^2 = (E^2 e^{-2\gamma(u)} - M_z^2 e^{-2\xi(u)} - L^2 e^{-2\beta(u)} - \iota) \exp[-2(\beta(u) + \gamma(u) + \xi(u))] \equiv f(u). \quad (14)$$

We write Eq. (14) in the form of an energy conservation law [17]

$$\dot{u}^2 e^{2[\beta(u)+2\gamma(u)+\xi(u)]} + \iota e^{2\gamma(u)} + M_z^2 e^{2(\gamma(u)-\xi(u))} + L^2 e^{2(\gamma(u)-\beta(u))} = E^2,$$

or, in terms of an effective potential,

$$\dot{u}^2 e^{2[\beta(u)+2\gamma(u)+\xi(u)]} + V_{eff}^2(u) = E^2,$$

where E is the conserved energy and

$$V_{eff}(u) = \sqrt{\iota e^{2\gamma(u)} + M_z^2 e^{2(\gamma(u)-\xi(u))} + L^2 e^{2(\gamma(u)-\beta(u))}} \quad (15)$$

is the effective potential for the geodesic motion.

By virtue of (13) Eqs. (7), (9), and (10) are satisfied identically, and Eq. (8) is a differential consequence of Eq. (14). We rewrite Eq. (8) in the form

$$\ddot{u} = -(\gamma' + \beta' + \xi')f(u) - E^2 \gamma' e^{-2\gamma(u)} + M_z^2 \xi' e^{-2\xi(u)} + L^2 \beta' e^{-2\beta(u)} \exp[-2(\beta(u) + \gamma(u) + \xi(u))]. \quad (16)$$

By integrating (14) and applying (13), we get functions $t = t(\tau)$, $u = u(\tau)$, $z = z(\tau)$, and $\phi = \phi(\tau)$ describing the classical (non-quantum) motion of uncharged point particle.

In the following sections we consider three possible cases: 1) $M_z = L = 0$, 2) $M_z = 0$, $L \neq 0$, and 3) $L = 0$, $M_z \neq 0$.

Non-zero components of Riemann curvature tensor $R_{\mu\nu\lambda\rho}$ of metric (3) are

$$\begin{aligned} R_{u\phi u\phi} &= -(h/4) \tanh(hu) (2|q_e| \cosh(hu))^{1/2} [h \tanh(hu) + b] e^{2au}, \\ R_{uzuz} &= -(h/4) \tanh(hu) (2|q_e| \cosh(hu))^{1/2} [h \tanh(hu) + a] e^{2bu}, \\ R_{tutu} &= -(h/4) (2|q_e| \cosh(hu))^{-1/2} [(3h/2) \tanh^2(hu) + (a+b) \tanh(hu) - h], \\ R_{z\phi z\phi} &= (h/4) (2|q_e| \cosh(hu))^{1/2} [(h/4) \tanh^2(hu) + (a+b) \tanh(hu) + h], \\ R_{t\phi t\phi} &= (h/4) (2|q_e| \cosh(hu))^{-1/2} [(h/4) \tanh^2(hu) + a \tanh(hu)] e^{-2bu}, \\ R_{tztz} &= (h/4) (2|q_e| \cosh(hu))^{-1/2} [(h/4) \tanh^2(hu) + b \tanh(hu)] e^{-2au}. \end{aligned}$$

From here we can calculate the Ricci tensor $R_\mu^\nu = g^{\nu\rho} R_{\rho\lambda\mu}^\lambda$ and scalar curvature $R = R_\mu^\mu$:

$$\begin{aligned} R_t^t &= -(h^2/4) (2|q_e|)^{-1/2} (\text{sech}(hu))^{5/2} e^{-2(a+b)u}, \\ R_u^u &= -(h^2/8) (2|q_e| \text{sech}(hu))^{1/2} [3 \tanh^2(hu) + 2(\text{sech}(hu))^2] e^{-2(a+b)u}, \\ R_z^z &= (h^2/4) (2|q_e|)^{-1/2} (\text{sech}(hu))^{5/2} e^{-2(a+b)u}, \\ R_\phi^\phi &= (h^2/4) (2|q_e|)^{-1/2} (\text{sech}(hu))^{5/2} e^{-2(a+b)u}, \\ R &= -(3h^2/8) (2|q_e| \text{sech}(hu))^{1/2} \tanh^2(hu) e^{-2(a+b)u}, \end{aligned}$$

and from these we can compute the Kretschmann invariant $K = R_{\mu\nu\lambda\rho}R^{\mu\nu\lambda\rho}$:

$$K = (1/4)|q_e|^{-5}[c_1 + c_2 \operatorname{sech}(hu) \sinh(hu) - c_3 \operatorname{sech}^2(hu) - c_4 \operatorname{sech}^3(hu) \sinh(hu) + 71h^4 \operatorname{sech}^4(hu)] \operatorname{sech}(hu) e^{-4(a+b)u},$$

where $c_1 = 24a^2b^2 + (2a^2 + 3ab + 2b^2)h^2 + (7/32)h^4$, $c_2 = (a+b)(8ab + h^2)h$, $c_3 = [2a^2 + 11ab + 2b^2 + (15/16)h^2]h^2$, and $c_4 = 3(a+b)h^3$.

It can be easily verified that $\lim_{u \rightarrow -\infty} K = +\infty$ (for $a, b > 0$). From here it follows that space-time (3) becomes singular as $r \rightarrow 0$ and has a physical singularity at $u = -\infty$ ($r = 0$) (for $a, b > 0$).

III. RADIAL MOTION OF MASSIVE TEST PARTICLES.

We consider the first case: $M_z = L = 0$. From (12) we have $z = \text{const}$ and $\phi = \text{const}$. Hence, only t and u can depend on τ . The motion in this case is called radial.

From Eqs. (4), (13)–(16) one can obtain the following equations for time-like geodesics:

$$t = t_0 + E\sqrt{2|q_e|} \int_{\tau_1}^{\tau_2} \sqrt{\cosh(hu(\bar{\tau}))} d\bar{\tau}, \quad z(\tau) = z_0, \quad \phi(\tau) = \phi_0,$$

$$\dot{u}^2 = P_{rm}(E, u) e^{-2(a+h^2/(4a))u}, \quad (17)$$

$$\ddot{u} = S_{rm}(E, u) e^{-2(a+h^2/(4a))u}, \quad (18)$$

$$V_{eff}(u) = \frac{1}{\sqrt[4]{2|q_e|} \cosh(hu)},$$

where we have denoted

$$P_{rm}(E, u) \equiv E^2 - \frac{1}{\sqrt{2|q_e|} \cosh(hu)}, \quad S_{rm}(E, u) \equiv \frac{h}{4} \frac{\tanh(hu)}{\sqrt{2|q_e|} \cosh(hu)} - (a + h^2/(4a))P_{rm}(E, u).$$

The plot of the effective potential $V_{eff}(u)$ for radial timelike geodesics in space-time (3) at fixed $h = 1$, $q_e = 0.5$, and $a = 0.125$ is shown in Fig. 1.

It follows from Eq. (17) that the function $P_{rm}(E, u)$ must be nonnegative

$$P_{rm}(E, u) = E^2 - \frac{1}{\sqrt{2|q_e|} \cosh(hu)} \geq 0.$$

This condition is satisfied for all real $u \in (-\infty, +\infty)$ when $E \geq 1/\sqrt[4]{2|q_e|}$ and for $u \in (-\infty, u_-] \cup [u_+, +\infty)$ with

$$u_{\pm} = \pm h^{-1} \left| \operatorname{arcosh}[(2|q_e|E^4)^{-1}] \right| \quad (19)$$

when $E \leq 1/\sqrt[4]{2|q_e|}$.

The turning points of the particle motion are defined by equation $\dot{u} = 0$ or, by virtue of (17), by equation $P_{rm}(E, u) \exp[-2(a + h^2/(4a))u] = 0$. Solving this equation, we find $u = u_{\pm}$ or, in terms of the coordinate r ,

$$r_{\pm} = \left(\frac{1 \pm \sqrt{1 - 4q_e^2 E^8}}{2|q_e|E^4} \right)^{1/h} \quad (r_+ > 1, \quad r_- = 1/r_+ < 1). \quad (20)$$

The circle radii of the turning points are

$$\rho_{\pm} = \frac{1}{E} r_{\pm}^a.$$

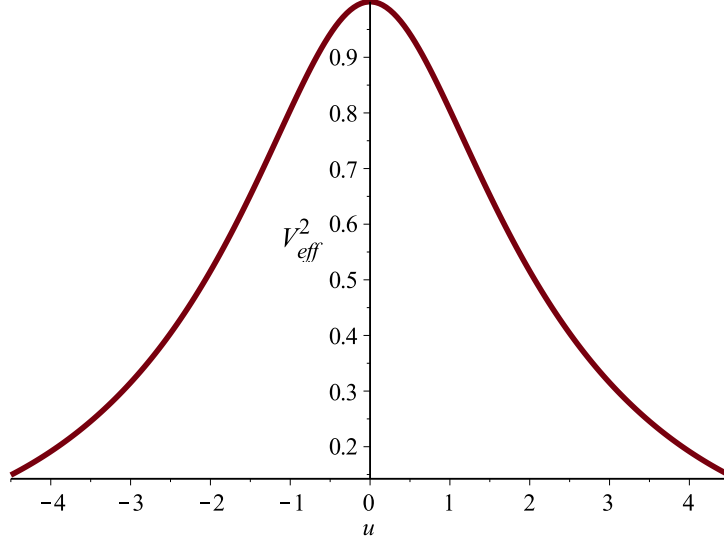


FIG. 1: The plot of the squared effective potential $V_{eff}^2(u)$ for radial timelike geodesics ($M_z = L = 0$) in space-time (3) at fixed $h = 1$, $q_e = 0.5$, and $a = 0.125$.

The regions accessible by a particle with energy E are $u \leq u_-$ ($r \leq r_-$) or $u \geq u_+$ ($r \geq r_+$). For a given $E < 1/\sqrt[4]{2|q_e|}$ there is a potential barrier at $u_- < u < u_+$ ($r_- < r < r_+$), whereas for $E > 1/\sqrt[4]{2|q_e|}$ the potential barrier vanishes.

A value of E may be chosen such that u_- and u_+ coincide, and the potential barrier vanishes. Equating u_- and u_+ , we find $u = 0$ ($r = 1$), $E = 1/\sqrt[4]{2|q_e|} \equiv E_0$, and from (17), (18) it follows that $\dot{u}|_{u=0} = 0$, $\ddot{u}|_{u=0} = 0$. The particle located at $u = u_- = u_+ = 0$ ($r = 1$) will be at a point of unstable equilibrium. Actually, the only equilibrium point $u = 0$ ($r = 1$) along radial timelike geodesics is found by solving the equation $V'_{eff}(u) = 0$. The equilibrium is unstable, since $V''_{eff}(0) = -(1/4)h^2/\sqrt[4]{2|q_e|} < 0$, and the effective potential V_{eff} has a maximum at $u = 0$.

We consider trajectories of particles with $E < E_0$ moving from the turning points u_+ or u_- . It follows from (18) that initial accelerations at the turning points are

$$\ddot{u}_{\pm} \equiv \ddot{u}(u_{\pm}) = \pm(hE^2/4)\sqrt{1 - 4q_e^2 E^8} e^{-2(a+h^2/(4a))u_{\pm}}.$$

The initial acceleration is positive for u_+ and negative for u_- . A particle starting from rest at u_+ moves away from the singularity at $u = -\infty$ ($r = 0$), and a particle that starts from rest at u_- moves in the opposite direction and falls into this singularity in a finite proper time. Namely, for the latter particle we have from (17)

$$\begin{aligned} \frac{d\tau}{du} &= -\exp[(a + h^2/(4a))u] \left(E^2 - E_0^2/\sqrt{\cosh(hu)} \right)^{-1/2}, \\ \tau &= \frac{1}{E_0} \int_{-\infty}^{u_-} \frac{\exp[(a + h^2/(4a))u] \sqrt[4]{\cosh(hu_-) \cosh(hu)}}{\left(\sqrt{\cosh(hu)} - \sqrt{\cosh(hu_-)} \right)^{1/2}} du = \\ &= \frac{1}{\sqrt[4]{2}E_0} \int_0^{r_-} \frac{\sqrt[4]{(r_-^h + r_-^{-h})(r^h + r^{-h})}}{r^{1-a-h^2/(4a)} \left(\sqrt{r^h + r^{-h}} - \sqrt{r_-^h + r_-^{-h}} \right)^{1/2}} dr < +\infty, \end{aligned} \quad (21)$$

whereas we expressed the particle energy E in terms of the initial value u_{\pm} (r_{\pm}) of the radial coordinate by using Eqs. (19), (20):

$$E = \frac{E_0}{\sqrt[4]{\cosh(hu_{\pm})}} = \frac{\sqrt[4]{2}E_0}{\sqrt[4]{r_{\pm}^h + r_{\pm}^{-h}}}.$$

We also assumed that $\tau = 0$ at the starting point $u_- < 0$ ($r_- < 1$) and took into account the series expansion

$$\sqrt{r^h + r^{-h}} - \sqrt{r_-^h + r_-^{-h}} = \frac{h}{2r_-} \frac{r_-^h - r_-^{-h}}{\sqrt{r_-^h + r_-^{-h}}} (r - r_-) + o(r - r_-).$$

Similarly, for the particle that starts from rest at $u_+ > 0$ ($r_+ > 1$) we have

$$\tau = \frac{1}{\sqrt[4]{2E_0}} \int_{r_+}^{+\infty} \frac{\sqrt[4]{(r_+^h + r_+^{-h})(r^h + r^{-h})}}{r^{1-a-h^2/(4a)} \left(\sqrt{r^h + r^{-h}} - \sqrt{r_+^h + r_+^{-h}} \right)^{1/2}} dr = +\infty.$$

The particle starting from rest at $u_+ > 0$ ($r_+ > 1$) is separated by the potential barrier from the singularity at $u = -\infty$ ($r = 0$). It moves away from the singularity and reaches infinity in infinite proper time $\tau = +\infty$.

In order that a radially moving particle with energy $E < E_0$ could traverse or touch the wormhole throat $u = u_0 < 0$ ($r = r_0 < 1$) it must be that $u_- \geq u_0$ ($r_- \geq r_0$). Due to Eqs. (5), (19), this is equivalent to the following condition:

$$-|\operatorname{arcosh}[(2|q_e|E^4)^{-1}]| \geq -\operatorname{arctanh}(4a/h).$$

From here we find a (lower) *energy threshold* E_{thr} of traversability of the wormhole throat for a radially moving massive test particle:

$$E \geq E_{thr} \equiv E_0 \sqrt[8]{1 - 16a^2/h^2} \quad (E_0 = 1/\sqrt[4]{2|q_e|}). \quad (22)$$

Radially moving particles starting from rest at $u_- > u_0$ with energy E satisfying $E_{thr} < E < E_0$ pass through the throat and fall to the singularity in a finite proper time. Radial trajectories of massive particles starting from rest at $u_- < u_0$ with energy $E < E_{thr}$ do not pass through the wormhole throat.

Massive particles with energy $E = E_{thr}$ start at the turning point $u_- = u_0$ on the wormhole throat and fall to the singularity in a finite proper time.

Radially moving particles with energy $E < E_0$ that start from rest at u_+ do not traverse the wormhole throat; they move away from the throat and reach infinity in infinite proper time.

In the case $2|q_e|E^4 > 1$, i. e., when $E > E_0$, the right-hand side of (17) is strictly positive and $\dot{u} \neq 0$ for all real u . A particle with an initial value u_i of the radial coordinate and positive initial radial velocity $\dot{u}_i = \dot{u}(u_i) > 0$ moves away from the singularity and reaches infinity in infinite proper time. If $u_i < u_0$, the particle crosses the wormhole throat in a finite proper time $\tau = \int_{u_i}^{u_0} (d\tau/du) du$. In the case of negative initial radial velocity $\dot{u}_i < 0$ the particle moves toward the singularity, crosses the wormhole throat in a finite proper time $\tau = \int_{u_0}^{u_i} (d\tau/du) du$ (only if $u_i > u_0$), and falls to the singularity in a finite proper time $\tau = \int_{-\infty}^{u_i} (d\tau/du) du$ (see Eq. (21)). Thus, for $E > E_0$ the wormhole is traversable for radially moving test particles with non-zero rest masses.

To obtain information about the possible modes of behavior of particles in the last case $2|q_e|E^4 = 1$, i. e., when $E = E_0$, we rewrite Eqs. (17), (18) in the form of the dynamical system

$$\dot{u} = s, \quad \dot{s} = \frac{h \tanh(hu) \exp[-2(a + h^2/(4a))u]}{4 \sqrt{2|q_e|} \cosh(hu)} - (a + h^2/(4a))s^2, \quad (23)$$

and study the nature and stability of the corresponding fixed points in the phase plane (u, s) . They are given by the equations $\dot{u} = \dot{s} = 0$ whose solution is the only fixed point $(0, 0)$. The corresponding Jacobian matrix J about the fixed point $(0, 0)$ has the form

$$J(0, 0) = \begin{pmatrix} 0 & 1 \\ G_0 & 0 \end{pmatrix}, \quad G_0 = (1/4)h^2 E_0^2.$$

Its eigenvalues $l_{\pm} = \pm(1/2)hE_0$ are real and distinct. Therefore, the fixed point $(0, 0)$ is an unstable saddle point. A typical phase portrait of dynamical system (23) at fixed $h = 1$, $q_e = 0.5$, $a = 0.125$ is presented in Fig. 2.

A particle with energy E_0 and initial values $u_i < 0$, $\dot{u}_i < 0$ moves toward the singularity, crosses the wormhole throat (only if $u_i > u_0$) and falls to the singularity in a finite proper time

$$\tau = \frac{1}{E_0} \int_{-\infty}^{u_i} \frac{\exp[(a + h^2/(4a))u]}{(1 - \sqrt{\operatorname{sech}(hu)})^{1/2}} du.$$

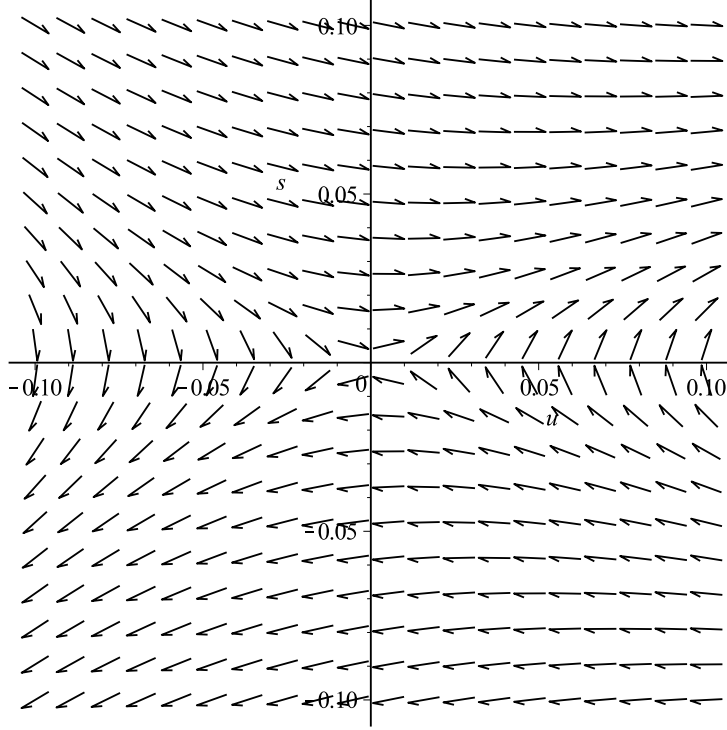


FIG. 2: The phase portrait of dynamical system (23) at fixed $h = 1$, $q_e = 0.5$, $a = 0.125$.

If $u_i < 0$, but $\dot{u}_i > 0$, the particle moves to the hypersurface $u = 0$ and reaches it in infinite proper time due to the divergence of the integral $\int_{u_i}^0 (d\tau/du) du$ at $u = 0$, which is evident from the series expansion $1 - 1/\sqrt{\cosh(hu)} = (1/4)h^2u^2 + o(u^3)$.

A particle with energy E_0 and initial values $u_i > 0$, $\dot{u}_i > 0$ moves away from the singularity and reaches infinity in infinite proper time $\int_{u_i}^{+\infty} (d\tau/du) du$. In the case $u_i > 0$, $\dot{u}_i < 0$ the particle moves to the hypersurface $u = 0$ and reaches it in infinite proper time $\int_0^{u_i} (d\tau/du) du$, so the particle does not cross the throat. It turns out that the hypersurface $u = 0$ traps out particles with energy E_0 .

IV. RADIAL MOTION OF PHOTONS.

From Eq. (14) for null geodesics $\iota = 0$ it follows that

$$\dot{u}^2 = (E^2 e^{-2\gamma} - M_z^2 e^{-2\xi} - L^2 e^{-2\beta}) e^{-2(\gamma+\beta+\xi)}.$$

Since we consider radial geodesics, we put $M_z = L = 0$, and the equation takes the form

$$\dot{u}^2 = E^2 e^{-2(2\gamma+\beta+\xi)}$$

or, in view of (4), the form

$$\dot{u}^2 = E^2 e^{-2(a+h^2/(4a))u}.$$

Integrating, we find

$$u(\tau) = (a + b)^{-1} \ln[\pm(a + h^2/(4a))E(\tau - \tau_0)].$$

The radial coordinate u varies from $-\infty$ to $+\infty$ if $\dot{u} > 0$ (outgoing radial null geodesics) or from $+\infty$ to $-\infty$ if $\dot{u} < 0$ (ingoing radial null geodesics). Each of such geodesics crosses the throat, and the wormhole turns out to be traversable by photons.

V. NON-RADIAL MOTION IN THE PLANE $z = \text{const}$ ($M_z = 0$).

In the case $M_z = 0$, $L \neq 0$ we obtain from (12) $z = \text{const}$, hence, particles move along a hypersurface $z = \text{const}$ (“planar orbits”). From Eqs. (4), (14), (15), and (16) we obtain

$$\dot{u}^2 = \left(E^2 - E_0^4 L^2 e^{-2au} \text{sech}(hu) - \iota E_0^2 \sqrt{\text{sech}(hu)} \right) e^{-2(a+b)u}, \quad (24)$$

$$\begin{aligned} \ddot{u} = & \left((1/4)\iota h E_0^2 \tanh(hu) \sqrt{\text{sech}(hu)} + \right. \\ & \left. (1/2) E_0^4 L^2 \text{sech}(hu) (h \tanh(hu) + 2a) e^{-2au} - (a+b)P(u) \right) e^{-2(a+b)u}, \\ V_{eff}^2(u) = & E_0^2 \left(E_0^2 L^2 e^{-2au} \text{sech}(hu) + \iota \sqrt{\text{sech}(hu)} \right). \end{aligned} \quad (25)$$

The plot of the effective potential $V_{eff}(u)$ for timelike geodesics ($\iota = 1$) in the plane $z = \text{const}$ ($M_z = 0$) at fixed $L = 1$, $E_0 = 1$, $h = 1$, $a = 1/8$ is shown in Fig. 3.

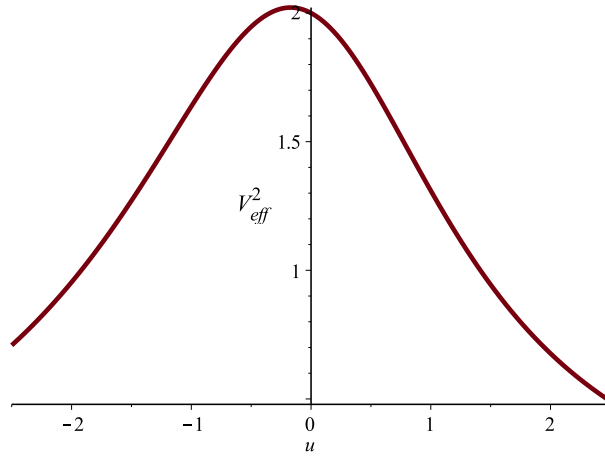


FIG. 3: The plot of $V_{eff}^2(u)$ (25) for timelike geodesics ($\iota = 1$) in the plane $z = \text{const}$ ($M_z = 0$) at fixed $L = 1$, $E_0 = 1$, $h = 1$, $a = 1/8$.

By considering u as a function of ϕ and combining Eqs. (12) and (24), we derive the equation

$$\begin{aligned} \left(\frac{du}{d\phi} \right)^2 = & E_0^{-4} L^{-2} \left(E^2 - E_0^4 L^2 e^{-2au} \text{sech}(hu) - \iota E_0^2 \sqrt{\text{sech}(hu)} \right) \cosh(hu) e^{2(a-b)u} \\ \equiv & E_0^{-4} L^{-2} P(u) \cosh(hu) e^{2(a-b)u}. \end{aligned} \quad (26)$$

Once this equation has been solved, the complete solution can be obtained by direct quadratures of the equations

$$\frac{d\tau}{d\phi} = (\sqrt{E_0}/L) \sqrt{\cosh(hu)} e^{2au} \quad \text{and} \quad \frac{dt}{d\phi} = (EE_0/L) \cosh(hu) e^{2au}.$$

In asymptotic regions, when $u \rightarrow \pm\infty$, we get $P(u) \rightarrow E^2 - 0$. It follows from Eq. (26) that for the large enough positive values of the coordinate u we have approximately

$$\left| \frac{du}{d\phi} \right| = \frac{1}{\sqrt{2E_0^2|D|}} e^{(h/2+a-b)u}$$

or, after integration,

$$e^{-(h/2+a-b)u} = \frac{1}{\sqrt{2E_0^2|D|}} |(h/2+a-b)(\phi - \phi_{+\infty})|, \quad \phi_{+\infty} = \text{const},$$

where we introduced an impact parameter $D = L/E$. Since $0 < a < h/4$ and $h/2 + a - b < 0$ (see Eq. (3)), this implies a spiral character of the particle motion at infinity $u = +\infty$, i.e., $\phi \rightarrow \phi_{+\infty}$ when $u \rightarrow +\infty$. By analogy, in the case when $u \rightarrow -\infty$, we get

$$e^{-(h/2+a-b)u} = \frac{1}{\sqrt{2E_0^2|D|}} |(-h/2 + a - b)(\phi - \phi_{-\infty})|, \quad \phi_{-\infty} = \text{const},$$

which, because of the condition $-h/2 + a - b < 0$, confirms the radial character of the motion near the singularity, i.e., $\phi \rightarrow \phi_{-\infty}$ when $u \rightarrow -\infty$.

The radii u_c (r_c) of circular orbits and the corresponding values of E and L are defined by extrema of $V_{eff}(u)$, namely, the minima correspond to stable orbits, while the maxima correspond to unstable orbits. The joint solution of equations $V_{eff}(u) = E$ and

$$V'_{eff}(u) = -(1/4)V_{eff}^{-1} \left(\iota h \tanh(hu) + 2E_0^2 L^2 (2a + h \tanh(hu)) e^{-2au} \sqrt{\text{sech}(hu)} \right) = 0$$

(which are equivalent to equations $P(u) = 0$ and $P'(u) = 0$) gives the only radius $u_c \leq -h^{-1} \text{arctanh}(2a/h)$ ($r_c \leq [(h-2a)/(h+2a)]^{1/(2h)}$), which is equal for null geodesics ($\iota = 0$) to

$$u_c = -h^{-1} \text{arctanh}(2a/h) \quad (r_c = [(h-2a)/(h+2a)]^{1/(2h)}),$$

and for timelike geodesics ($\iota = 1$) it is implicitly defined by the equation

$$2E_0^2 L^2 (2a + h \tanh(hu_c)) e^{-2au_c} \sqrt{\text{sech}(hu_c)} + h \tanh(hu_c) = 0.$$

Since $V''_{eff}(u_c) < 0$, the circular orbit $u = u_c$ is unstable. As V_{eff} has no finite minima, there are no stable circular orbits.

As for the radial motion, it can be verified that the fixed point $(u_c, 0)$ is an unstable saddle point of the corresponding dynamical system similar to system (23).

We will show that, as in the Kerr and Schwarzschild geometries, we should distinguish between orbits with impact parameters greater resp. less than a certain critical value D_c of the impact parameter, which corresponds to the unstable circular orbit of radius u_c (r_c). For $D^2 > D_c^2$ there are two kinds of orbits: orbits of the first kind arrive from infinity and have pericenter distances greater than u_c , whereas orbits of the second kind have apocenter distances less than u_c and terminate at the singularity at $u = -\infty$ ($r = 0$). For $D = D_c$ orbits of the first and second kinds merge, and both orbits spiral infinite number of times around the unstable circular orbit $u = u_c$. For $D^2 < D_c^2$ we have only orbits of one kind: starting at infinity, they cross the wormhole throat and terminate at the singularity.

As in the radial case, the geometry of the geodesics (photon and massive test particles orbits) is determined by the number and the location of the roots of the equation $P(u) = 0$.

It follows from the above that the function $V_{eff}^2(u)$ has the only maximum at $u = u_c$. Hence, the function

$$P(u) = L^2 (D^{-2} - V_{eff}^2(u)/L^2) \quad (27)$$

has the only minimum at u_c . Since $P(u)$ is smooth and its limit equals L^2/D^2 when u approaches $+\infty$ or $-\infty$, it has no more than two real zeros, which we denote by u_1 and $u_2 > u_1$. As a result, we have the following three cases described below.

Case (a): $P(u)$ has one zero at u_c . From $P(u_c) = 0$ we find the critical value of the impact parameter: $D_c^2 \equiv 1/U(u_c)$. Equation (26), where $P(u)$ is given by (27) and $D^2 = D_c^2$, has solution $u = u_c$, which is the unstable circular orbit at u_c . Expanding this equation to second order in $u - u_c$ and neglecting terms of higher order, we obtain

$$\left(\frac{du}{d\phi} \right)^2 = \alpha^2 (u - u_c)^2 \quad (\alpha = \text{const} > 0)$$

(where for photon orbits $\alpha^2 = (1/2)(h-2a)^{1-b/h}(h+2a)^{b/h}$) or, in the integrated form,

$$(i) \ u = u_c + e^{\pm\alpha(\phi-\phi_0)}, \ u > u_c \quad (ii) \ u = u_c - e^{\pm\alpha(\phi-\phi_0)}, \ u < u_c.$$

Eq. (i) shows that $u \rightarrow u_c + 0$ when $\phi \rightarrow \mp\infty$, i.e., an orbit asymptotically approaches the circle at u_c spiraling around it in clockwise or in counter-clockwise directions an infinite number of times. This is an

orbit of the first kind. In the interior of the circular orbit $u = u_c$, one obtains orbits of the second kind. Derived from Eq. (ii), they unwind from the circular orbit and fall to the singularity.

For the null geodesics (the photon orbits) the function $P(u)$ (see Eq. (24) and Eq. (26)) becomes

$$P(u) \equiv L^2 (D^{-2} - E_0^4 e^{-2au} \text{sech}(hu)),$$

$$\left(\frac{du}{d\phi}\right)^2 = E_0^{-4} (D^{-2} - E_0^4 e^{-2au} \text{sech}(hu)) \cosh(hu) e^{2(a-b)u}, \quad (28)$$

or, in the coordinate r ,

$$\left(\frac{dr}{d\phi}\right)^2 = \frac{1}{2} D^{-2} E_0^{-4} r^{2(a-b+1)} (r^h + r^{-h}) - r^{2(1-b)}.$$

The photon orbits $u = u(\phi)$ of the first kind are shown in Fig. 4 by the solid line and those of the second kind by the dashed line. Since $u_{th} \equiv -h^{-1} \text{arctanh}(4a/h) < u_c \equiv -h^{-1} \text{arctanh}(2a/h)$, the photon orbits of the first kind cannot cross the throat, but the photon orbits of the second kind can traverse the throat.

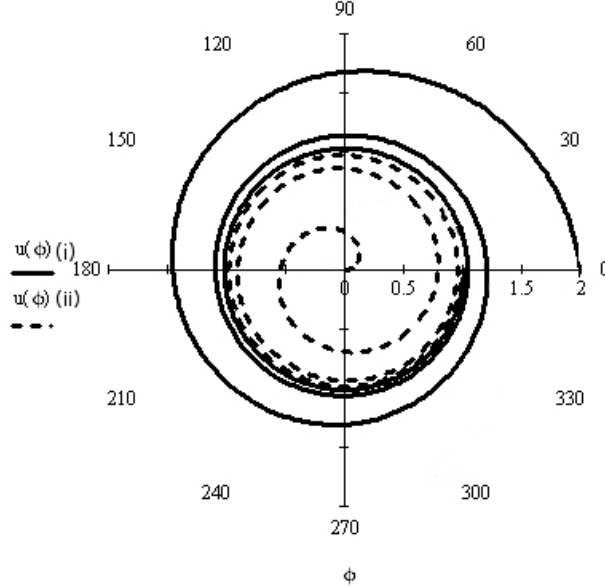


FIG. 4: The photon orbits $u = u(\phi)$ of the first kind (the solid line) and the second kind (the dashed line) in the plane $z = \text{const}$ for $D^2 = D_c^2$.

Case (b): $P(u)$ has no zeros, i. e., $P(u) > 0$ for all $u \in \mathbb{R}$. We use Eq. (27) to rewrite Eq. (26) in the form

$$\left(\frac{du}{d\phi}\right)^2 = E_0^{-4} D_c^{-2} (D_c^2/D^2 - U(u)/U(u_c)) e^{2(a-b)u} \cosh(hu). \quad (29)$$

Taking into account that $U(u)$ has maximum $U(u_c)$ at u_c and, hence, $0 < U(u)/U(u_c) \leq 1$ for all u , we see that $D_c^2/D^2 > 1$, i. e., $D^2 < D_c^2$. The radial coordinate varies from $-\infty$ to $+\infty$, and $du/d\phi$ vanishes nowhere. Thus, particles starting at infinity cross the wormhole throat and fall to the singularity, so the wormhole is traversable.

Case (c): $P(u)$ has two real zeros u_1, u_2 and $u_1 < u_c < u_2$. This is possible only if $D^2 > D_c^2$. For every value of the impact parameter D there exist two distinct orbits confined to the intervals $u \leq u_1$ and $u \geq u_2$, respectively. They are derived from the expansion of Eq. (29) in the neighbourhoods of points u_1 and u_2 , namely,

$$(du/d\phi)^2 = \pm \alpha^2 (u - u_{1,2}) + o(u - u_{1,2}), \quad \alpha = \text{const} > 0.$$

Neglecting higher-order terms and integrating, we get orbits of the first kind $u = u_2 + \alpha(\phi - \phi_0)^2$, $u \geq u_2$, arriving from infinity and having pericenter distance u_2 and the orbits of the second kind $u = u_1 - \alpha(\phi - \phi_0)^2$, $u \leq u_1$, having the apocenter distance u_1 and terminating at a singularity at $u = -\infty$ ($r = 0$).

VI. NON-RADIAL MOTION IN THE PLANE $\phi = \text{const}$ ($L = 0$).

In the case $M_z \neq 0$, $L = 0$ it follows from (12) that $\phi = \text{const}$, so particles move along a hypersurface (“plane”) $\phi = \text{const}$. As in the preceding section we have from Eqs. (4), (14), (15), and (16)

$$\left(\frac{du}{d\tau}\right)^2 = \left(E^2 - \iota E_0^2 \sqrt{\text{sech}(hu)} - E_0^4 M_z^2 e^{-2bu} \text{sech}(hu)\right) e^{-2(a+b)u} \equiv \tilde{P}(u) e^{-2(a+b)u} \quad (30)$$

or

$$\left(\frac{du}{d\tau}\right)^2 = (E^2 - V_{eff}^2(u)) e^{-2(a+b)u},$$

where

$$V_{eff}^2(u) = E_0^2 \left(\iota \sqrt{\text{sech}(hu)} + E_0^2 M_z^2 e^{-2bu} \text{sech}(hu) \right) \quad (31)$$

is the squared effective potential shown for timelike geodesics ($\iota = 1$) in Fig. 5.

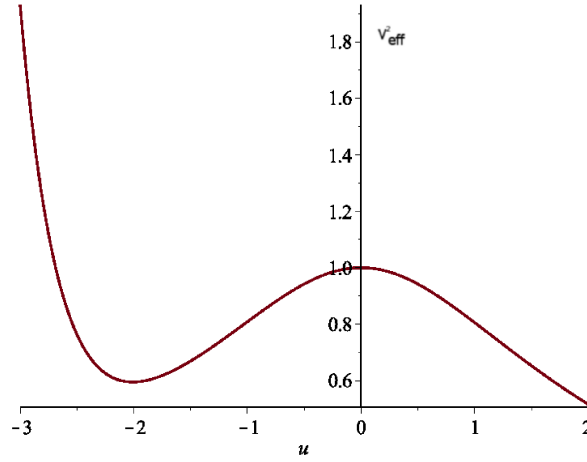


FIG. 5: The plot of $V_{eff}^2(u)$ (31) for timelike geodesics ($\iota = 1$) in the plane $\phi = \text{const}$ ($L = 0$) at fixed $M_z = 10^{-2}$, $E_0 = 1$, $h = 1$, $a = 1/8$, $b = 2$.

Eqs. (12) and (30) give

$$\left(\frac{du}{dz}\right)^2 = E_0^{-4} M_z^{-2} \tilde{P}(u) \cosh(hu) e^{2(b-a)u}. \quad (32)$$

The complete solution of the last equation is obtained by quadratures of the equations

$$\frac{d\tau}{dz} = \frac{1}{E_0^2 M_z} \sqrt{\cosh(hu)} e^{2bu} \quad \text{and} \quad \frac{dt}{dz} = \frac{E}{E_0^4 M_z} \cosh(hu) e^{2bu}.$$

Eqs. (30) and (32) for large values of u ($u \rightarrow +\infty$) imply

$$\left(\frac{du}{dz}\right)^2 = \frac{1}{2} E_0^{-4} H^{-2} e^{(2b-2a+h)u}, \quad H \equiv M_z/E,$$

$$\left(\frac{du}{d\tau}\right)^2 = E^2 e^{-2(a+b)u}$$

or, in the integrated form,

$$e^{-(h/2+b-a)u} = -\frac{1}{\sqrt{2E_0^2|H|}} (h/2 + b - a)(z - z_{+\infty}),$$

$$e^{(a+b)u} = E(a+b)(\tau - \tau_0).$$

Since $h/2 + b - a > 0$, it follows that $z \rightarrow z_{+\infty} - 0 \neq +\infty$ and $\tau \rightarrow +\infty$ when $u \rightarrow +\infty$, which means that particles reach (radial) infinity in infinite proper time.

The extrema of the effective potential $V_{eff}(u)$ define the radii u_c of orbits: the minima (resp., the maxima) correspond to stable (resp., unstable) orbits. The joint solution of the equations $V_{eff}(u) = E$ (or $\tilde{P}(u) = 0$) and $V'_{eff}(u) = 0$ (or $\tilde{P}'(u) = 0$) gives a radius u_c , that determines a fixed point of Eq. (30). Calculating the first derivative of $V_{eff}(u)$, we get

$$V'_{eff}(u) = -(1/4)V_{eff}^{-1} \left(\iota h \tanh(hu) \sqrt{\text{sech}(hu)} + 2E_0^2 M_z^2 (2b + h \tanh(hu)) e^{-2bu} \sqrt{\text{sech}(hu)} \right).$$

For null orbits ($\iota = 0$) the equation $V'_{eff}(u) = 0$ has no real roots, since $2b/h > 1$, and the function $\tilde{P}(u) = E^2 - V_{eff}^2(u)$ has the only zero at u_1 . Consequently, all null orbits have a pericenter distance u_1 and terminate at radial infinity.

For timelike orbits ($\iota = 1$) the equation $V'_{eff}(u) = 0$, which can be written in the form

$$\tanh(hu) = -\frac{2[b/h]}{(2M_z^2 E_0^2)^{-1} \exp(2bu) \sqrt{\cosh(hu)} + 1},$$

can allow no more than two real roots. Therefore, the equation $V_{eff}(u) = E$ (or $\tilde{P}(u) = 0$) can allow no more than three real roots. Since $\lim_{u \rightarrow +\infty} \tilde{P}(u) = E^2 > 0$ and $\lim_{u \rightarrow -\infty} \tilde{P}(u) = -\infty$, the equation $\tilde{P}(u) = 0$ must always have at least one real root. Thus, we have to distinguish between the following four cases (see Fig. 6).

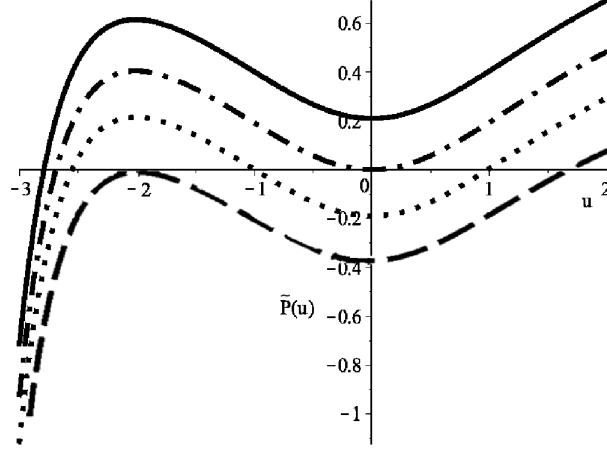


FIG. 6: Disposition of zeros of the function $\tilde{P}(u)$ in the case of timelike geodesics at fixed $M_z = 10^{-2}$, $E_0 = 1$, $h = 1$, $a = 1/8$, $b = 2$, $E = 1.1$ (the solid line), $E = 1.0$ (the dash-dotted line), $E = 0.9$ (the dotted line), $E = 0.77$ (the dashed line).

Case (a): $\tilde{P}(u)$ has three distinct real zeros at u_1, u_2, u_3 : $u_1 < u_2 < u_3$ (the dotted line in Fig. 6). There exist two kinds of orbits. An orbit of the first kind oscillates between two values of u with u_1 being a pericenter and u_2 an apocenter. An orbit of the second kind arrives from infinity and has the pericenter distance u_3 .

Case (b): $\tilde{P}(u)$ has two distinct real zeros at u_1, u_2 : $u_1 < u_2$, $\tilde{P}'(u_1) \neq 0$, $\tilde{P}'(u_2) = 0$. Then $\tilde{P}(u)$ has a minimum and $V_{eff}(u)$ has a maximum at u_2 (the dash-dot line in Fig. 6). We have the unstable orbit $u = u_2$. The orbit of the first kind starts at the pericenter distance u_1 and approaches the orbit $u = u_2$ asymptotically in infinite proper time. The orbit of the second kind arrives from infinity and has the pericenter distance u_2 .

Case (c): $\tilde{P}(u)$ has two distinct real zeros at u_1, u_2 : $u_1 < u_2$, $\tilde{P}'(u_1) = 0$, $\tilde{P}'(u_2) \neq 0$. Then $\tilde{P}(u)$ has a maximum and $V_{eff}(u)$ has a minimum at u_1 (the dashed line in Fig. 6). We have a stable orbit $u = u_1$ and an orbit that arrives from infinity and has the pericenter distance u_2 .

Case (d): $\tilde{P}(u)$ has one zero at u_1 (the solid line in Fig. 6). Orbits arrive from infinity and have the pericenter distance u_1 .

VII. CONCLUSION

We studied the radial and non-radial motion of test particles for cylindrically symmetric wormholes of type WhCR^e found earlier [5] in the 6-dimensional reduced Kaluza–Klein theory with the Abelian gauge field and two dilaton fields. We showed that space–time (3) has a regular wormhole region and has a physical singularity at $u = -\infty$ (for $a, b > 0$). The motion of test particles in the ϕ and z -direction is governed by two conserved conjugate momenta L and M , and the radial motion is described by an effective potential as in Fig. 1. This potential is repulsive away from the wormhole throat region. This difference from the typically attractive nature of spherically symmetric wormholes is related to the collapse of the latter, which allows a particle at the throat to move to a smaller circle radius, whereas in our example the size of the throat does not change. Thus, for a radially moving particle with energy $E < 1/\sqrt[4]{2|q_e|}$ there is a potential barrier at $u_- < u < u_+$. Equating u_- and u_+ gives $u = 0$, $E = 1/\sqrt[4]{2|q_e|} \equiv E_0$, so the particle located at $u = u_- = u_+ = 0$ will be at a point of (unstable) equilibrium. The energy E_0 divides motions of qualitatively different behavior. The particle with energy $E < E_0$ starting from rest at $u_+ > 0$ is separated by the potential barrier from the singularity at $u = -\infty$. It moves away from the singularity and reaches infinity in infinite proper time $\tau = +\infty$. In order that a radially moving particle with energy $E < E_0$ could traverse or touch the wormhole throat $u = u_0 < 0$ it must have $u_- \geq u_0$. From this follows the existence of a (lower) energy threshold $E_{thr} \equiv E_0 \sqrt[8]{1 - 16a^2/h^2}$ of traversability of the wormhole throat for a radially moving massive test particle. Particles starting from rest at $u_- > u_0$ with energy E satisfying $E_{thr} < E < E_0$ pass through the throat and fall to the singularity in a finite proper time.

Radial trajectories of massive particles starting from rest at $u_- < u_0$ with energy $E < E_{thr}$ do not pass through the wormhole throat. Massive particles with energy $E = E_{thr}$ start at the point of rest $u_- = u_0$ on the wormhole throat and fall toward the singularity in a finite proper time. Radially moving particles with energy $E < E_0$ that start from rest at u_+ do not traverse the wormhole throat; they move away from the throat and reach infinity in infinite proper time. For $E > E_0$ the wormhole is traversable for radially moving test particles with non-zero rest masses.

A particle with energy E_0 and initial values $u_i < 0, \dot{u}_i < 0$ of radial coordinate and velocity moves toward the singularity, crosses the wormhole throat (only if $u_i > u_0$) and falls to the singularity in a finite proper time. If $u_i < 0$, but $\dot{u}_i > 0$, the particle moves to the hypersurface $u = 0$ and reaches it in infinite proper time. When $u_i > 0, \dot{u}_i > 0$ a particle moves away from the singularity and reaches infinity in infinite proper time. In the case $u_i > 0, \dot{u}_i < 0$ the particle moves toward the hypersurface $u = 0$ and reaches it in infinite proper time, so the particle does not cross the throat (the hypersurface $u = 0$ traps out particles with energy E_0). Photons, being scale (conformally) invariant, cannot have a critical energy E_0 , and in fact we found that each radial photon trajectory crosses the throat.

In the case of non-radial motion the effective potential has a “centrifugal potential” contribution due to the conserved canonical momenta M and L of the z - and ϕ -motion. As shown by Eq (19), this contribution is always positive, and therefore increases the potential barrier compared to that for pure radial motion. For motion in the hypersurface $z = \text{const}$ (“planar orbits”, $M = 0, L \neq 0$) the ability of a particle to overcome this barrier can be stated in terms of its impact parameter D . As in the Kerr and Schwarzschild geometries we should then distinguish, [17], between orbits with impact parameters greater and/or less than a certain critical value D_c of the impact parameter, which corresponds to the unstable circular orbit of radius u_c (r_c). For $D^2 > D_c^2$ there are two kinds of orbits: orbits of the first kind arrive from infinity ($u = +\infty$) and have pericenter distances greater than u_c , whereas orbits of the second kind have apocenter distances less than u_c and terminate at singularity at $u = -\infty$. For $D = D_c$ orbits of the first and second kinds spiral infinite number of times on the unstable circular orbit $u = u_c$. For $D^2 < D_c^2$ we have only orbits of one kind: starting at infinity, they cross the wormhole throat and terminate at the singularity. Thus, to penetrate the wormhole, improperly (non-radially) aimed planar orbits need more energy and time to traverse the wormhole, but they still do not avoid the central singularity.

In the case of non-radial motion in the plane $\phi = \text{const}$ the effect of the corresponding “centrifugal potential” due to M is similar to that due to L except that V_{eff} always diverges at $u = -\infty$, shielding the singularity: all orbits have a finite pericenter distance. All null orbits have a pericenter distance u_1 and terminate at radial infinity. For massive particles we have to distinguish between the four cases (a, b, c, d). In case (a) there exist two kinds of orbits: an orbit of the first kind oscillates between two values of u with u_1 being a pericenter and u_2 an apocenter, an orbit of the second kind arrives from infinity and has the pericenter distance $u_3 > u_2 > u_1$. In case (b) we have the unstable orbit $u = u_2$; the orbit of the first kind starts at the pericenter distance $u_1 < u_2$ and approaches the orbit $u = u_2$ asymptotically in the infinite proper time, and the orbit of the second kind arrives from infinity and has the pericenter distance u_2 . In case (c) we have the stable orbit at $u = u_1$ and an orbit that arrives from infinity and has the pericenter distance

$u_2 > u_1$. In case (d) orbits arrive from infinity and have the pericenter distance u_1 . This type of orbit allows traversing the wormhole from V_+ , spending a finite time on the "other side" V_- without encountering the singularity, and reemerging in the original space V_+ .

-
- [1] M. Cvetič and D. Youm, Nucl. Phys. B, **438**, 182 (1995); Addendum-ibid. **449**,146 (1995); arXiv:hep-th/9409119 [hep-th].
 - [2] M. Cvetič and D. Youm, Phys. Rev. D **52**, 2144 (1995)]
 - [3] K. A. Bronnikov and J. P. S. Lemos, Phys. Rev. D **79**, 104019 (2009).
 - [4] M. S. Morris and K. S. Thorne, Am. J. Phys. **56** (5), 395 (1988).
 - [5] A. V. Aminova and P. I. Chumarov, Phys. Rev. D **88**, 044005 (2013).
 - [6] M. Visser, *Lorentzian wormholes: from Einstein to Hawking*, (AIP Press. New York, 1995).
 - [7] M. S. Morris, K. S. Thorne, U. Yurtsever, Phys. Rev. Lett. **61**, 1446 (1988).
 - [8] P. E. Kashargin and S. V. Sushkov, Grav. Cosmol. **14**, 80 (2008).
 - [9] V. Kagramanova and E. Smolarek, arXiv:1302.1705 [gr-qc].
 - [10] N. J. Popławski, Phys. Lett. B **687**, 110 (2010).
 - [11] E. Hackmann and H. Xi, Phys. Rev. D **87**, 124030 (2013).
 - [12] T. Matos, Gen. Rel. Grav. **42**, 1969 (2010).
 - [13] T. Matos, L. Arturo Ureña-López, G. Miranda, arXiv:1203.4801v2 [gr-qc].
 - [14] G. Miranda, T. Matos, N. Motelongo García, arXiv:1303.2410v1 [gr-qc].
 - [15] C. G. Böhrer, T. Harko, and V. Sabau, Adv. Theor. Math. Phys. **16**, 1145-1196 (2012).
 - [16] K. A. Bronnikov, J. Phys. A: Math. Gen. **12**, 201 (1979).
 - [17] S. Chandrasekhar, *The mathematical theory of black holes*, (Oxford University Press, New York, 1983).
 - [18] E. Poisson, A. Pound, I. Vega, arXiv:1102.0529v3 [gr-qc].